CHIN. PHYS. LETT. Vol. 38, No. 6 (2021) 066201

New Members of High-Energy-Density Compounds: YN_5 and YN_8

Jun-Yi Miao(苗俊一)[1,2], Zhan-Sheng Lu(路战胜)[1], Feng Peng(彭枫)[2,1*], and Cheng Lu(卢成)[3*]

[1]*School of Physics, Henan Normal University, Xinxiang 453007, China*
[2]*College of Physics and Electronic Information, Luoyang Normal University, Luoyang 471022, China*
[3]*School of Mathematics and Physics, China University of Geosciences (Wuhan), Wuhan 430074, China*

(Received 11 March 2021; accepted 6 April 2021; published online 25 May 2021)

Polymeric nitrogen is a promising candidate for a high-energy-density material. Synthesis of energetic compounds with high chemical stability under ambient conditions is still a challenging problem. Here we report a theoretical study on yttrium nitrides by first principles calculations combined with an effective crystal structure search method. It is found that many yttrium nitrides with high nitrogen content can be formed under relatively moderate pressures. The results indicate that the nitrogen-rich YN_5 and YN_8 compounds are recoverable as metastable high-energy materials under ambient conditions, and can release enormous energies ($2.51\,\mathrm{kJ\cdot g^{-1}}$ and $3.18\,\mathrm{kJ\cdot g^{-1}}$) while decomposing to molecular nitrogen and YN. Our findings enrich the family of transition metal nitrides, and open avenues for design and synthesis of novel high-energy-density materials.

DOI: 10.1088/0256-307X/38/6/066201

Exploration of novel high-energy-density materials (HEDMs) in polynitrogen form has attracted significant attention for decades due to its important applications, such as energy storage, rocket propellants and explosives. Polynitrogen materials become ideal HEDM candidates because they are "green" energetic materials and exhibit a uniquely large difference in energies between different phases consisting of single bonds and triple bonds.[1] Generally, nitrogen is a diatomic N_2 molecule with a strong triple N≡N bond under ambient conditions.[2] An effective method to break the extremely strong triple N≡N bond and to obtain polymeric nitrogen is using high pressure.[3] In this direction, the predicted single-bonded frameworks of cubic gauche (cg-N) has been synthesized successfully at high pressure (110 GPa) and high temperature (2000 K).[3,4] Very recently, the layered Pba_2 (LP-N) structure has been observed.[5,6] However, both cg-N and LP-N are just metastable at pressures above 42 GPa at room temperature[3] and the ultrahigh pressure required to stabilize them has precluded their practical applications.

To reduce the synthesis pressure of single-bonded polymeric nitrogen, many works have focused on searching the novel polymeric nitrogen materials by introducing other elements into "precompressing" N_2. A reliable research tool for screening HEDM candidates is pressing, and thereby will avoid expensive and dangerous experimental tests. Many metal nitrides,[7−14] and nonmetal nitrides[15−18] are predicted. Recently, Raza *et al.*[19] have found that N_2 can react with carbon monoxide at pressures above 52 GPa. While relieving the pressure to the ambient pressure, the corresponding compound maintains its three-dimensional (3D) covalent frame-work and is dynamically stable.[19] The underlying mechanism of the reduced stabilization pressure might be attributed to the chemical precompression resulting from other elements,[20] the existence of more types of N–N bonds than the N_2 molecule,[21] or the assistance of additional chemical bonds between N and other elements.

Synthesis of polynitrogen materials requires elimination of N_2-like molecular units. One feasible method is to introduce electrons which are favored by N_2 molecules and which occupy the empty antibonding σ^* orbitals of N_2 molecules, thus weakening the intramolecular N–N bonds and dissociation of the N_2 isomer. Recent work reported that the MgN_{10} compound can be stable at high pressure since two N_5 anions accept $2e$ from the magnesium atom,[22] while LiN_5 can be stable due to $1e$ charge transfer of $Li\rightarrow N_5$.[7] The more the electrons are obtained, the higher the nitrogen content in the compound can be achieved. Therefore, rare earth (RE) nitrides have entered our research perspectives. Normally, RE elements, such as Y metal, can easily lose electrons because of their small electronegativities in the range of 1.0–1.36 on the Pauli scale,[23] which is comparable to that of Mg metal with a value of 1.0. Moreover, the RE elements accommodate higher oxidation states more easily (e.g., in 3^+ or 4^+) than that of Mg (2^+) in MgN_{10}, which enables donation of more electrons to the nitrogen molecules.

In this work, we carry out an extensively structural search of yttrium nitrides in a large pressure range from 0 to 100 GPa using the swarm-structure searching algorithm in conjunction with first-principles calculations.[24,25] Our results show

Supported by the National Natural Science Foundation of China (Grant Nos. 11774140, U1804121, and 11304167), and China Postdoctoral Science Foundation (Grant No. 2016M590033).
*Corresponding authors. Email: fpeng@calypso.cn; lucheng@calypso.cn
© 2021 Chinese Physical Society and IOP Publishing Ltd

that nitrogen can react with Y at a relatively low pressure (about 10 GPa) and form high-energy-density compounds with various compositions. The structures are diverse, including one-dimensional polymeric crystals such as YN_4/YN_5 and three-dimensional extended solid such as YN_8. Most importantly, the three-dimensional YN_8 shows a surprisingly high energy density of about 3.18 $kJ{\cdot}g^{-1}$, which is the highest nitride among all the known polynitrogen compounds, making YN_8 a promising candidate for HEDM.

Our structural searches are carried out using the particle swarm optimization (PSO) method as implemented in the CALYPSO code,[24–26] which is based on a global minimization of free energy surfaces obtained from *ab initio* total-energy calculations. It is specially designed for global structural minimization unbiased by any known structural information. This method has been benchmarked on various known systems, ranging from elements to binary and ternary compounds.[27–35] Total energy calculations are calculated by density functional theory (DFT) within the generalized gradient approximation[36] as implemented in the Vienna *ab initio* simulation package (VASP).[37] The Perdew–Burke–Ernzerhof (PBE)[38] functionals and the projector-augmented wave (PAW) method[39] are adopted in the structural optimizations. The $4s^2 4p^6 5s^2 4d^1$ and $2s^2 2p^3$ are treated as valence electrons for Y and N atoms, respectively. The energy cutoff of 900 eV and the adequate k-point sampling are chosen to ensure the excellent convergence of total energies. To obtain the stable pressure range for Y–N compounds, we calculated the formational enthalpies of all the chemical reaction channels for stable stoichiometries and the pure solid Y and N_2. Phonon calculations are calculated by the Phonopy code.[40]

The thermodynamic stability of Y–N systems with different stoichiometries of YN_x [$x = 1/4, 2/7, 1/3, 2/5, 1/2, 1, 3/2, 2, 5/2$, and 3–12] are thoroughly examined by comparing the formation enthalpies[29] at pressures of 0, 25, 50, 75 and 100 GPa, relative to the dissociation into solid Y and N_2, as shown by the convex hull [Fig. 1(a)]. The results show that YN is the most stable system at both high pressure and ambient pressure. This is consistent with the experiment, where only YN compounds with cubic structure can form at ambient pressure.[41] Figure 1(a) also indicates that the N content of the thermodynamically stable stoichiometries tends to rise with increasing pressure. In the low-pressure range (< 25 GPa), Y_5N_2, YN_3, YN_4 and YN_{10} are all stable besides the most stable YN. Unexpectedly, besides YN, YN_3, YN_4 and YN_{10}, YN_5 and YN_8 are also stable stoichiometries in the moderate pressure range about 75 GPa. Up to high pressure ranges (> 100 GPa), the stable stoichiometries are Y_3N_2, YN, YN_2, YN_3, YN_5, and YN_8.

To explore the dynamic stability of these nine newly uncovered Y-N compounds, we calculate their phonon dispersions (see Figs. S1–S9 in the Supplementary Material). The calculated phonon dispersions show no imaginary vibrational modes over the Brillouin zone, confirming the dynamic stabilities of these compounds. Thus, they are thermodynamically stable under the corresponding pressure range. The shift of the phase stability towards N-rich compositions with increasing pressure is accompanied by a series of structural changes promoted by variations in N–N bonding patterns. With increasing N content, the bonding patterns of N evolve from isolated N anion (Y_5N_2, Y_3N_2 and YN) to anionized N_4 (YN_2) and N_6 (YN_3), one-dimensional (1D) polynitrogens (YN_4 and YN_5), two-dimensional (2D) polynitrogens (YN_8) and eventually N_5 rings (YN_{10}).

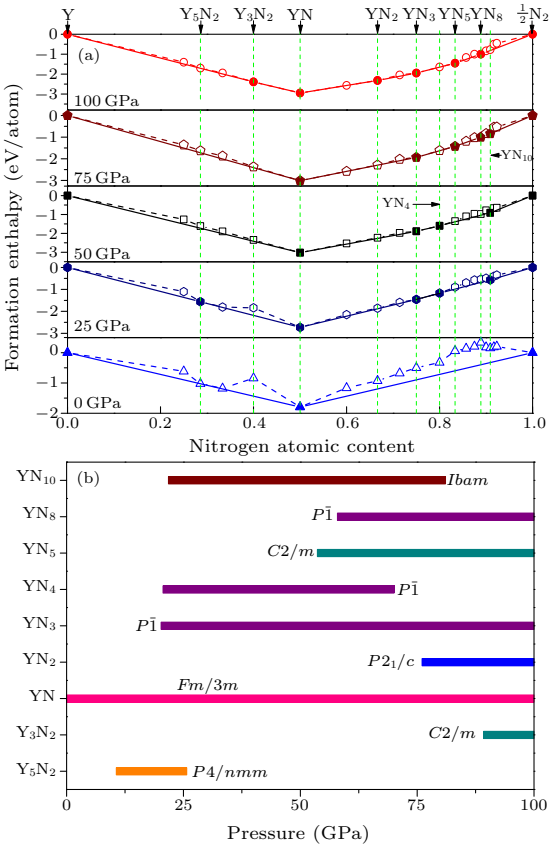

Fig. 1. (a) The convex hull of yttrium nitrides under different pressures. (b) The predicted stable pressure ranges of yttrium nitrides.

Y_5N_2, the Y rich nitride, is a layered structure with tetragonal $P4/nmm$ symmetry [see Fig. S10(a) in the Supplementary Material] at 25 GPa. The structure parameters are listed in Tables S1–S2 in the Supplementary Material. Y_5N_2 contains two YN layers, one Y double layer and one quadruple layer of Y. The nitrogen in Y_5N_2 is absolutely reduced to isolated N anions in YN layers. The isolated N anion is a common configuration in alkali metal and alkali earth metal nitrides, such as Li_3N or Ca_2N.[23,24] Bader charge analysis[42] [see Fig. S11 in the Supplementary Material] reveals only a part of the charge ($1.47e$) of the Y atom transfer to the N atom in YN layers and a few

charge transfers of Y→ N in the layers of Y. In addition, a part of the valence charges of the Y atom are located in the interstices in the Y layers, which is confirmed by the electron localization function (ELF)[43] [see Fig. S12(a) in the Supplementary Material], and the other valence charges of the Y atom are looked upon as free electrons confirmed by the metallic characters from the electronic band structure and electronic density of states (DOS) calculations (see the Supplementary Material, Fig. S13).

Y_3N_2 is a monoclinic structure with $C2/m$ symmetry at 100 GPa [see Fig. S10(b) in the Supplementary Material] and the structure parameters are listed in Tables S1 and S2 in the Supplementary Material. It consists of Y cations and isolated N anions, which is verified by ELF [see Fig. S12(b) in the Supplementary Material]. Bader charge analysis, as shown in Fig. S11 in the Supplementary Material, reveals that some charge, about 1.14e, of the Y atom transfers to the N atom, and the other valence charges are free electrons, leading to its metallic character.

YN is a typical cubic $Fm\bar{3}m$ structure in the considered pressure range. The crystal structure parameters are present in Fig. S10(c) and Tables S1 and S2 in the Supplementary Material. Bader charge analysis (see the Supplementary Material, Fig. S11) reveals that 1.71e of the Y atom transfer to the N atom. The electronic band structure and DOS calculations (see the Supplementary Material, Fig. S14) show that YN is a weak metal. Generally, the chemical bonds of RE metal nitrides are a mixture of ionicity and covalent characters due to their d orbitals. However, the average distance between Y and N atoms in most Y–N compounds is about 2.51 Å, which is much larger than the sum of the covalent radii of Y (1.61 Å) and N (0.71 Å) atoms. It leads to the weak covalent character of Y–N bonds.

YN_2 adopts the monoclinic $P21/c$ structure [see the Supplementary Material, Fig. S10(d) and Tables S1 and S2] at 100 GPa, which contains N_4 anions and Y cations due to the charge transfer (1.81e) of Y→N. Previous reports show similar N_4 anions in the high pressure phases of CsN[8] and CaN.[9] The calculated electronic band structure and DOS, as shown in Fig. S15 in the Supplementary Material, visibly display the metallic character of YN_2. The N–N distances in YN_2 under 100 GPa are about 1.39 Å and 1.40 Å, which are close to the typical N–N bond lengths of single bond (1.45 Å) and double bond (1.25 Å).

YN_3 is a triclinic $P\bar{1}$ structure [see the Supplementary Material, Fig. S10(e)]. It is thermodynamically stable above 20.21 GPa [Fig. 1(b)]. It consists of N_6 anions and Y cations. The neutral N_6 molecule is a chained diazide geometry. However, the N_6 anion in YN_3 is a double U geometry with opposite direction and edge-sharing [see the Supplementary Material, Fig. S10(e)–S10(b)]. The calculated N–N distance of YN_3 under 50 GPa is 1.32 Å.

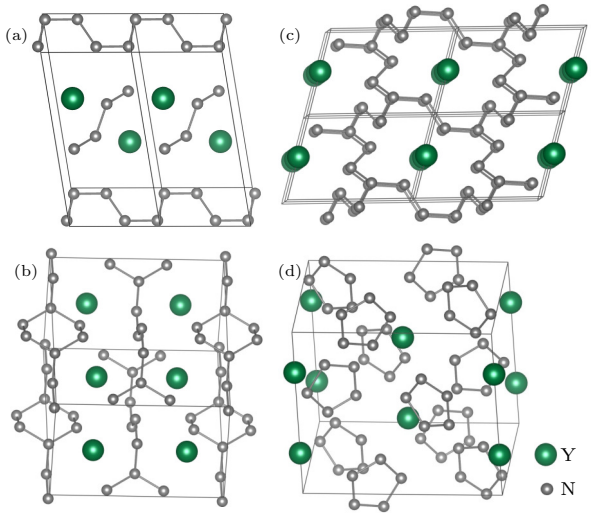

Fig. 2. Crystal structures of polynitrogens in yttrium nitrides. (a) The $P\bar{1}$ phase of YN_4 at 50 GPa. (b) The $C/2m$ structure of YN_5 at 100 GPa. (c) The polymeric $P\bar{1}$ phase at 75 GPa for YN_8. (d) Puckered plane N_5 ring *Ibam* phase of YN_{10} at 75 GPa.

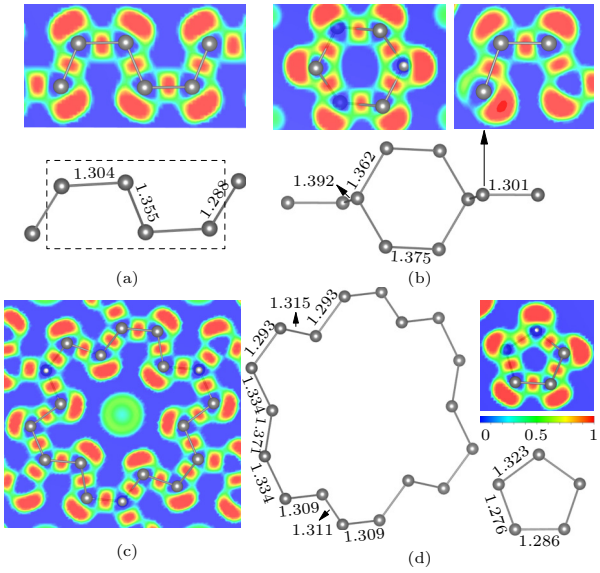

Fig. 3. ELFs and units of polynitrogens of yttrium nitrides. (a) The $P\bar{1}$ phase of YN_4 at 50 GPa. ELF plots in (0.34,0,1) sections for N_4 unit. (b) The $C/2m$ structure of YN_5 at 100 GPa. ELF plots in (0.65,0,−1) sections for N_{10} unit. (c) The polymeric $P\bar{1}$ phase of YN_8 at 75 GPa. ELF plots in (−1,−1,1) sections for N_{18} unit. (d) The puckered plane N_5 ring in *Ibam* phase of YN_{10} at 75 GPa. ELF plots in (0.48,1,0.3) sections for N_5 unit.

YN_4 is stable at pressures above 20.62 GPa [see Fig. 1(b)], with $P\bar{1}$ symmetry. The N atoms in YN_4 form 1D infinite chains, as shown in Fig. 2(a). The smallest unit contains four N atoms with a zigzag shape, which contains 1 single bond and 3 double bonds, i.e., [–N=N–N=N=]. The calculated N–N distances are 1.30, 1.36, 1.30, and 1.29 Å, respectively. The equal bonding nature of N_4 is confirmed by the ELF map [see Fig. 3(a)]. Interestingly, the similar repeated N_4 units are reported in our recent study[9] of

CaN_4 under high pressure. Moreover, the electronic band structure calculations of the $P\bar{1}$ phase (see the Supplementary Material, Fig. S17) show that YN_4 is metallic with nonzero DOS near the Fermi level.

YN_5 is a $C2/m$ structure [see Fig. 2(b)], and it is stable above 53.65 GPa. The N atoms are flocked together with [–N_2–N_6–N_2–] anions [Fig. 3(b)]. Y atoms are the electron donors. N atoms are bonded by six σ bonds with six lone pairs in the N_6 anion puckered plane [Fig. 3(b)]. Outside the N_6 anion plane, there are more than six π electrons that form a series of π bonds, which are uniformly distributed in the six N atoms. The ELF reveals that the N_2 anions are bonded by a single bond, and the rest of the electrons are lone pairs. The N–N distances in the N_6 ring of YN_5 phase are 1.36 Å and 1.38 Å at 100 GPa, which are between the single bond length of 1.45 Å and the double bond length of 1.20 Å.[3] The ground state of YN_5 reveals that it is a semiconductor with a small energy gap of about 0.2 eV [Fig. 4(a)].

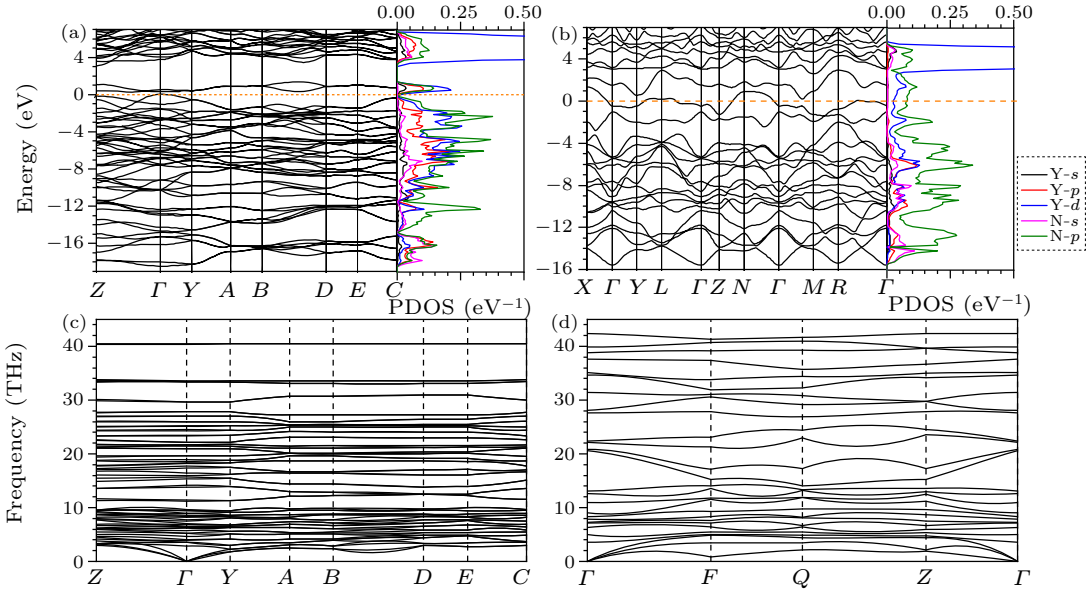

Fig. 4. Electronic band structure, DOS and phonon dispersion curves of yttrium nitrides. Band structures and DOS of $C2/m$ phase for YN_5 at 100 GPa (a) and $P\bar{1}$ phase of YN_8 at 75 GPa (b). Phonon dispersion curves of $C2/m$-YN_5 (c) and $P\bar{1}$-YN_8 (d) at ambient pressure.

YN_8 adopts a triclinic $P\bar{1}$ structure as shown in Fig. 2(c). It becomes thermodynamically stable above 57.95 GPa [see Fig. 1(b)]. The N atoms in YN_8 form 2D and puckered N_{18} rings with edge sharing, which are bonded by 18 σ bonds with 18 lone pairs outside the N atoms [Fig. 3(c)]. Meanwhile, there are more than 18 π electrons which constitute a number of π bonds that are unequally distributed in the 18 N atoms above and below the N_{18} rings. The layer nitrene is metallic due to the connection of π bonds confirmed by the ELF [Fig. 3(c)] and band structure [Fig. 4(b)] calculations. The DOSs [Fig. 4(b)] are primary N p states mixing with Y d states near the fermi level. The N–N distances in the N_{18} ring range from 1.29 Å to 1.37 Å at 75 GPa. Interestingly, the calculated T_c value is 3.3 K using Coulomb pseudopotential parameters (μ^*) with 0.1 for YN_8 at 75 GPa, which is the same behavior of TaN at high pressure.[44]

YN_{10} is an *Ibam* structure, as shown in Fig. 2(d). It is stable under pressure of at least 21.79 GPa. The N atoms inside are stacked as the N_5 anions [see Fig. 3(d)], and Y atoms are the electron donors. The N atoms, in the puckered plane N_5 anions, are bonded by five σ bonds concomitant with five lone pairs. More than five π electrons constitute a number of π bonds and are equally distributed between the five N atoms. The N–N distances in the N_5 anion are 1.28 Å, 1.33 Å and 1.29 Å at 75 GPa. It is noteworthy to mention that more than five π-electron N_5 rings disobey Hückel's rule, and the N_5 anion is unstable. Since the N_5 anion has additional electrons compared to its aromatic counterpart,[7,8] the ground state of YN_{10} is metallic (see Fig. S18 in the Supplementary Material).

The calculated elastic constants of $P2_1/c$-YN_4, $C2/m$-YN_5, $P\bar{1}$-YN_8, and *Ibam*-YN_{10} at ambient pressure are listed in Table S3 in the Supplementary Material.[45] It can be seen that the elastic constants of $P2_1/c$-YN4, $C2/m$-YN_5, and $P\bar{1}$-YN_8 obey the mechanical stability criteria of monoclinic and orthorhombic phases. However, the calculated elastic constants of *Ibam*-YN_{10} reveal that YN_{10} is unstable. The phonon dispersion curves at ambient pressure suggest that the YN_4 (see the Supplementary Material, Fig. S6)/YN_5 [Fig. 4(c)] with 1D nitrogen array and the YN_8 [Fig. 4(d)] with 2D nitrogen array are stable. Compared the structures of YN_4, YN_5 and YN_8 with other compounds, it can be seen that the N atoms in YN_4, YN_5 and YN_8 are polymerized into

N chains or N rings, which enhances the adhesion between the adjacent N atoms and improves their stability due to the strong covalent interactions. The above three metastable yttrium nitrides are expected to decompose exothermically to the products as solid YN and N, and we consider the decomposition reactions as follows:

$$YN_4 \rightarrow YN + 1.5N_2 + 1.97\,eV, \quad (1)$$

$$YN_5 \rightarrow YN + 2N_2 + 4.13\,eV, \quad (2)$$

$$YN_8 \rightarrow YN + 3.5N_2 + 6.63\,eV. \quad (3)$$

The chemical energies released during these reactions are estimated to be 1.97, 4.13, and 6.63 eV per YN_4, YN_5 and YN_8 unit at the GGA-PBE level, and the corresponding energy densities are approximately 1.31 $kJ{\cdot}g^{-1}$, 2.51 $kJ{\cdot}g^{-1}$, and 3.18 $kJ{\cdot}g^{-1}$. The highest energy density is YN_8, which is a good HEDM compared with conventional explosives, such as 1,3,5-triamino-2,4,6-trinitrobenzene (TATB), hexahydro-1,3,5-trinitro-1,3,5-triazine (RDX), and cyclotetramethylene tetranitramine (HMX) with the energy densities ranging from 1 to 5 $kJ{\cdot}g^{-1}$. [46]

In summary, we have predicted seven new stable yttrium nitrides under high pressure, including Y_5N_2/Y_3N_2 and YN phases with isolated N anions, YN_2 phase with anionic N_4, YN_3 phase with anionic N_6, YN_4/YN_5 phases with 1D polynitrogen array, YN_8 phase with 2D poly-nitrogen array and YN_{10} with N_5 rings array, by swarm-intelligence structure searches and first principles calculations. Phonon dispersion curve and formation enthalpy calculations suggest that the YN_4, YN_5 and YN_8 are metastable at ambient pressure. Most strikingly, YN_5 and YN_8, potentially recoverable at ambient pressure, can release enormous amounts of energy (about 2.51 $kJ{\cdot}g^{-1}$ and 3.18 $kJ{\cdot}g^{-1}$) while decomposing to solid YN and molecular nitrogen, making it a promising new HEDM compared to conventional explosives. These findings offer fundamental understanding of yttrium nitrides under high pressure, which provide powerful guidance for further design and synthesis of novel HEDMs.

One can see the Supplementary Material for details on the structural and electronic properties, phonon dispersion curves, and ELF curves of various yttrium nitrides under different pressures.

References

[1] Christe K O, Wilson W W, Sheehy J A and Boatz J A 1999 *Angew. Chem. Int. Ed.* **38** 2004
[2] Zahariev F, Dudiy S, Hooper J, Zhang F *et al.* 2006 *Phys. Rev. Lett.* **97** 155503
[3] Eremets M I, Gavriliuk A G, Trojan I A, Dzivenko D A *et al.* 2004 *Nat. Mater.* **3** 558
[4] Gregoryanz E, Goncharov A F, Sanloup C and Metal S 2007 *J. Chem. Phys.* **126** 184505
[5] Jiang S, Holtgrewe N, Lobanov S S, Su F, Mahmood M F *et al.* 2018 *Nat. Commun.* **9** 2624
[6] Lei L, Tang Q, Zhang F, Liu S *et al.* 2020 *Chin. Phys. Lett.* **37** 068101
[7] Peng F, Yao Y, Liu H and Ma Y 2015 *J. Phys. Chem. Lett.* **6** 2363
[8] Peng F, Han Y, Liu H and Yao Y 2015 *Sci. Rep.* **5** 16902
[9] Zhu S, Peng F, Liu H *et al.* 2016 *Inorg. Chem.* **55** 7550
[10] Shi X, Liu B, Yao Z and Liu B 2020 *Chin. Phys. Lett.* **37** 047101
[11] Ma S, Peng F, Zhu S, Li S *et al.* 2018 *J. Phys. Chem. C* **122** 22660
[12] Wang X, Li J, Zhu H, Chen L *et al.* 2014 *J. Chem. Phys.* **141** 044717
[13] Zhang M, Yan H, Wei Q, Wang H *et al.* 2013 *Europhys. Lett.* **101** 26004
[14] Steele B A, Stavrou E, Crowhurst J C, Zaug J M *et al.* 2017 *Chem. Mater.* **29** 735
[15] Peng F, Wang Y, Wang H, Zhang Y *et al.* 2015 *Phys. Rev. B* **92** 094104
[16] Yin K, Wang Y, Liu H, Peng F *et al.* 2015 *J. Mater. Chem. A* **3** 4188
[17] Li Y, Feng X, Liu H *et al.* 2018 *Nat. Commun.* **9** 722
[18] Steele B A and Oleynik I I 2017 *J. Phys. Chem. A* **121** 1808
[19] Raza Z, Pickard C, Pinilla C and Saitta A 2013 *Phys. Rev. Lett.* **111** 235501
[20] Ashcroft N W 2004 *Phys. Rev. Lett.* **92** 187002
[21] Prasad D L V K, Ashcroft N W and Hoffmann R 2013 *J. Phys. Chem. C* **117** 20838
[22] Xia K, Zheng X, Yuan J, Liu C *et al.* 2019 *J. Phys. Chem. C* **123** 10205
[23] Allred A L J 1961 *J. Inorg. Nucl. Chem.* **17** 215
[24] Wang Y, Lv J, Zhu L and Ma Y 2010 *Phys. Rev. B* **82** 094116
[25] Wang Y, Lv J, Zhu L and Ma Y 2012 *Comput. Phys. Commun.* **183** 2063
[26] Gao B, Gao P, Lu S, Lv J, Wang Y and Ma Y 2019 *Sci. Bull.* **64** 301
[27] Lv J, Wang Y, Zhu L and Ma Y 2011 *Phys. Rev. Lett.* **106** 015503
[28] Zhu L, Wang H, Wang Y, Lv J *et al.* 2011 *Phys. Rev. Lett.* **106** 145501
[29] Peng F, Miao M, Wang H, Li Q and Ma Y 2012 *J. Am. Chem. Soc.* **134** 18599
[30] Peng F, Sun Y, Pickard C J, Needs R J *et al.* 2017 *Phys. Rev. Lett.* **119** 107001
[31] Peng F, Song X, Liu C, Li Q *et al.* 2020 *Nat. Commun.* **11** 5227
[32] Lu C and Chen C 2020 *Phys. Rev. Mater.* **4** 043402
[33] Lu C and Chen C 2020 *Phys. Rev. Mater.* **4** 044002
[34] Sun W, Kuang X, Keen H D J, Lu C *et al.* 2020 *Phys. Rev. B* **102** 144524
[35] Chen B, Conway L J, Sun W, Kuang X *et al.* 2021 *Phys. Rev. B* **103** 035131
[36] Perdew J P and Wang Y 1992 *Phys. Rev. B* **45** 13244
[37] Perdew J P, Burke K and Ernzerhof M 1996 *Phys. Rev. Lett.* **77** 3865
[38] Kresse G and Furthmüller J 1996 *Phys. Rev. B* **54** 11169
[39] Blöchl P E 1994 *Phys. Rev. B* **50** 17953
[40] Togo A, Oba F and Tanaka I 2008 *Phys. Rev. B* **78** 134106
[41] Kempter C P, Krikorian N H and McGuire J C 1957 *Chem. Phys.* **61** 1237
[42] Bader R F W 1990 *Atoms in Molecules: A Quantum Theory* (Oxford: Clarendon)
[43] Becke A D and Edgecombe K E 1990 *J. Chem. Phys.* **92** 5397
[44] Jia Y, Zhao J, Zhang S, Yu S *et al.* 2019 *Chin. Phys. Lett.* **36** 087401
[45] Wu Z, Zhao E, Xiang H, Hao X *et al.* 2007 *Phys. Rev. B* **76** 054115
[46] Evans W J, Lipp M J, Yoo C S, Cynn H *et al.* 2006 *Chem. Mater.* **18** 2520

New members of high-energy-density compounds: YN_5 and YN_8

Jun-Yi Miao(苗俊一)[1,2] , Zhan-Sheng Lu(路战胜)[1], Feng Peng(彭枫) [2,1,*] and Cheng Lu(卢成)[3,*]

[1]School of Physics, Henan Normal University, Xinxiang, 453007, China
[2]College of Physics and Electronic Information, Luoyang Normal University, Luoyang 471022, China
[3]School of Mathematics and Physics, China University of Geosciences (Wuhan), Wuhan 430074, China

[a)] Electronic mail: fpeng@calypso.cn

[b)] Electronic mail: lucheng@calypso.cn

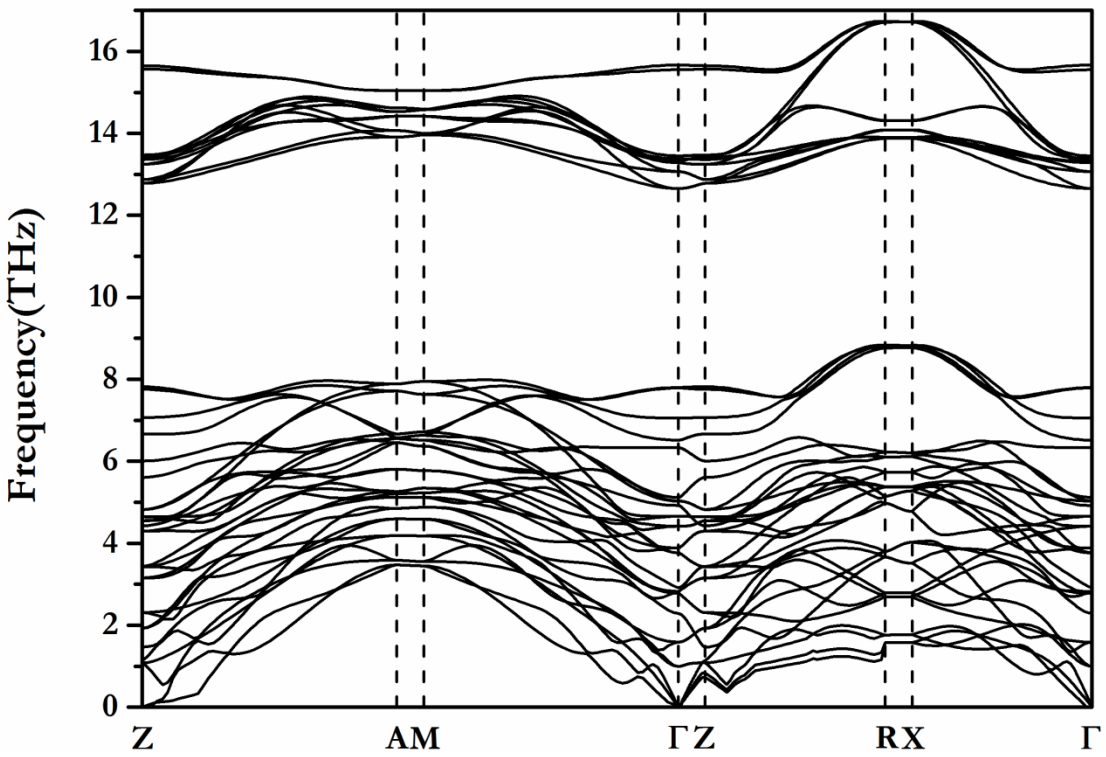

FIG. 1. Phonon dispersion curve of Y_5N_2 in the*P*4/*nmm* phase at 25 GPa

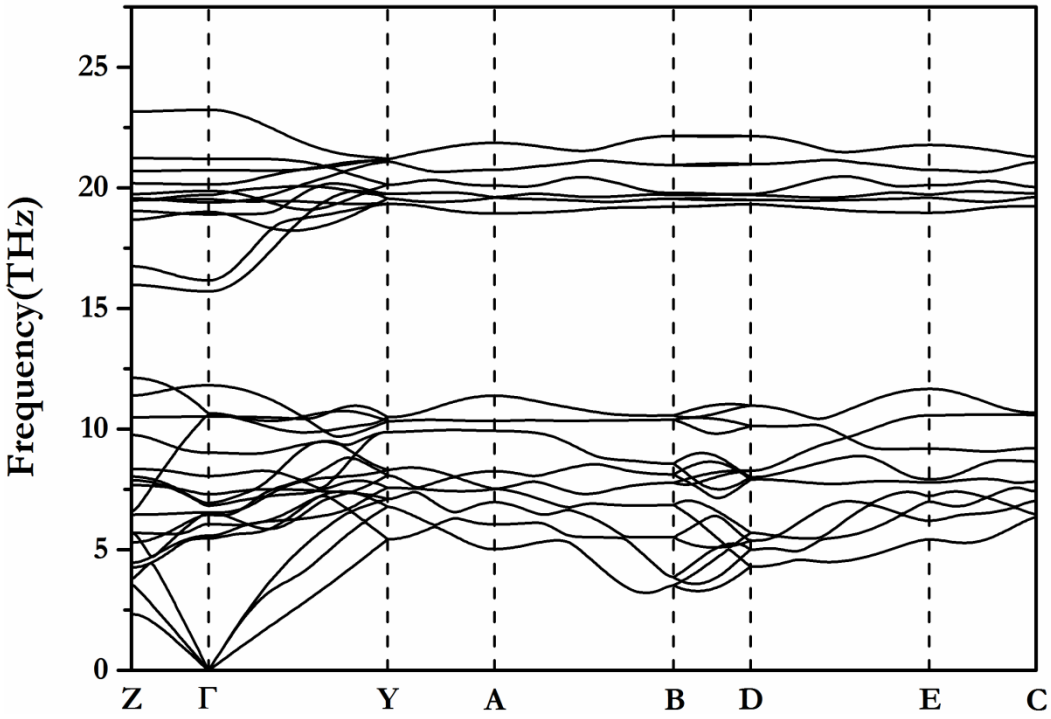

FIG. 2. Phonon dispersion curve of Y_3N_2 in the *C*2/*m* phase at 100 GPa.

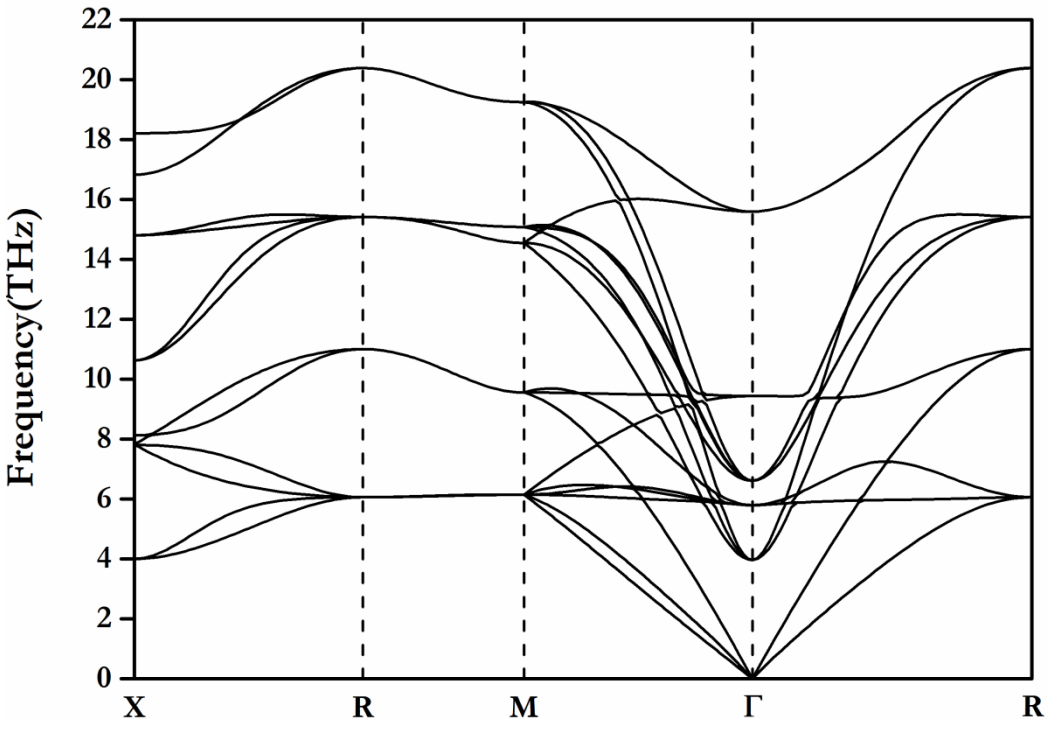

FIG. 3. Phonon dispersion curve of YN in the *Fm*-3*m* phase at 50 GPa.

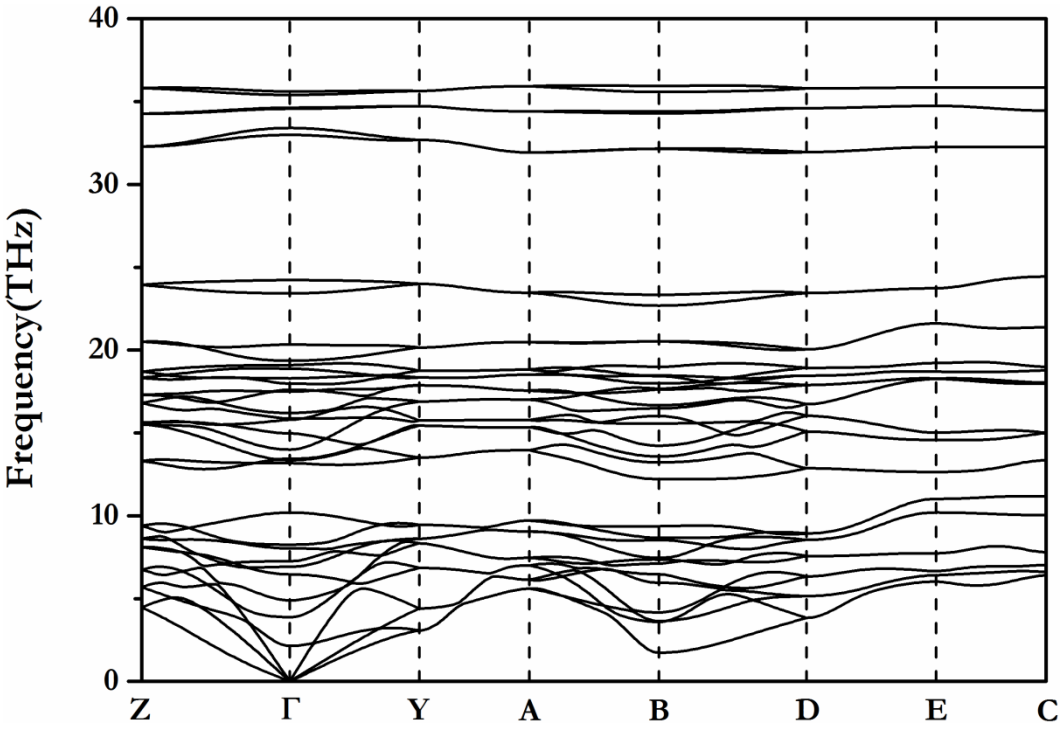

FIG. 4. Phonon dispersion curve of YN_2 in the $P2_1/c$ phase at 100 GPa.

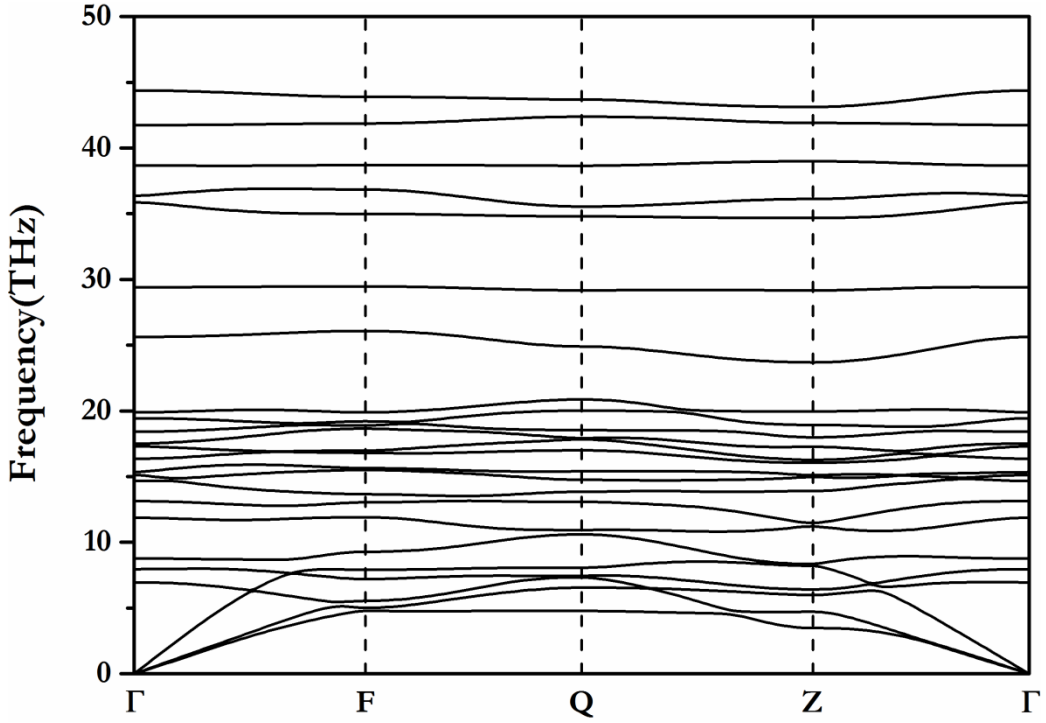

FIG. 5. Phonon dispersion curve of YN_3 in the P-1 phase at 50 GPa.

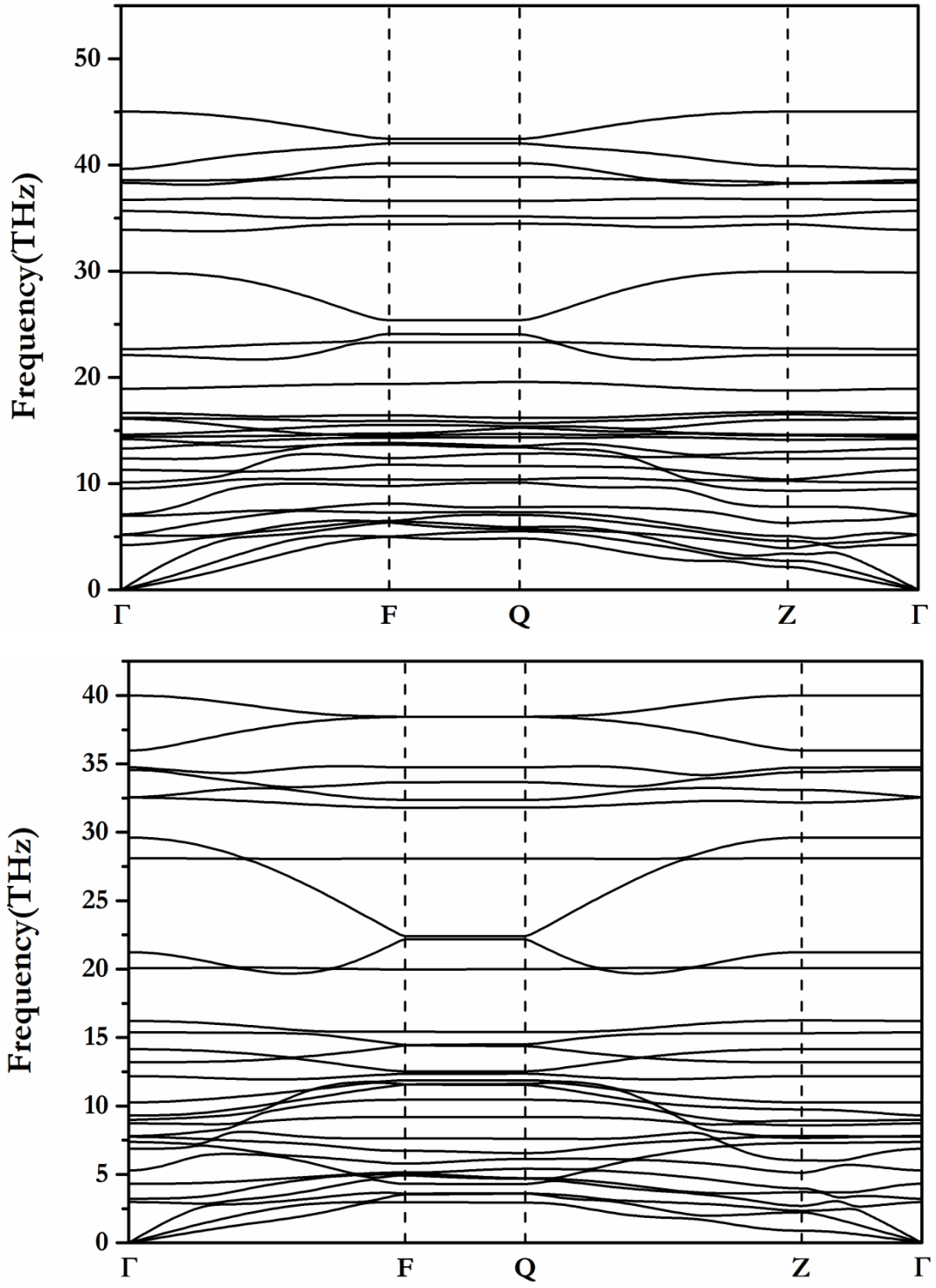

FIG. 6. Phonon dispersion curves of *P*-1 phase YN_4 at 50 GPa (upper panel) and 0 GPa (lower panel).

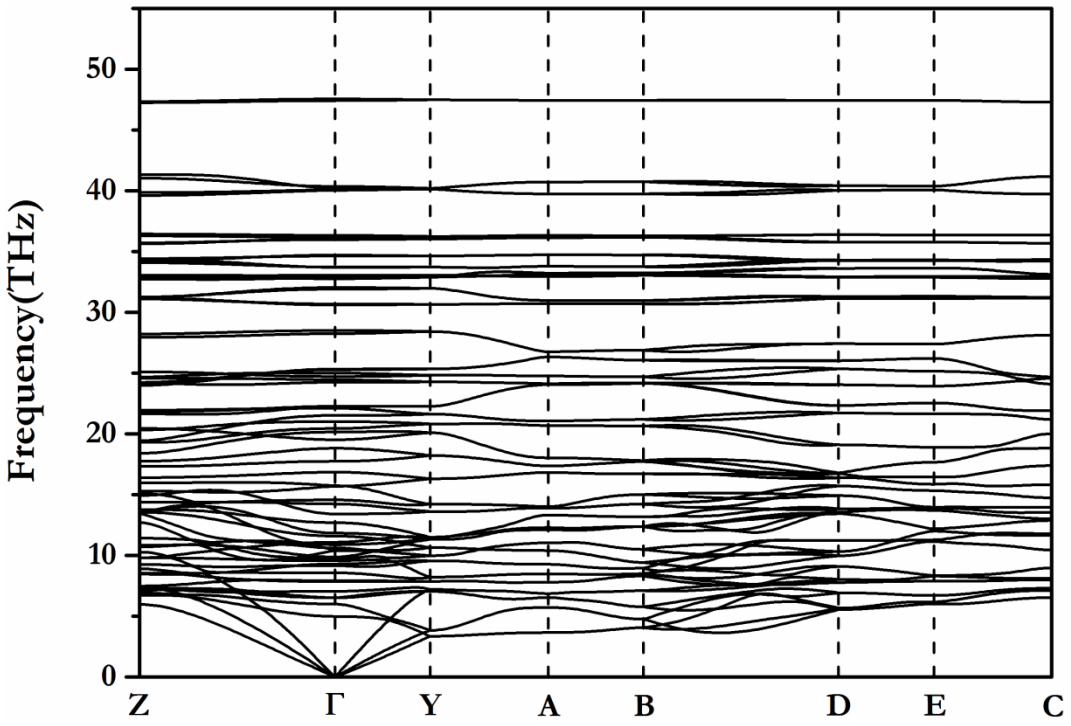

FIG. 7. Phonon dispersion curve of YN_5 in the *C*2/*m* phase at 100 GPa.

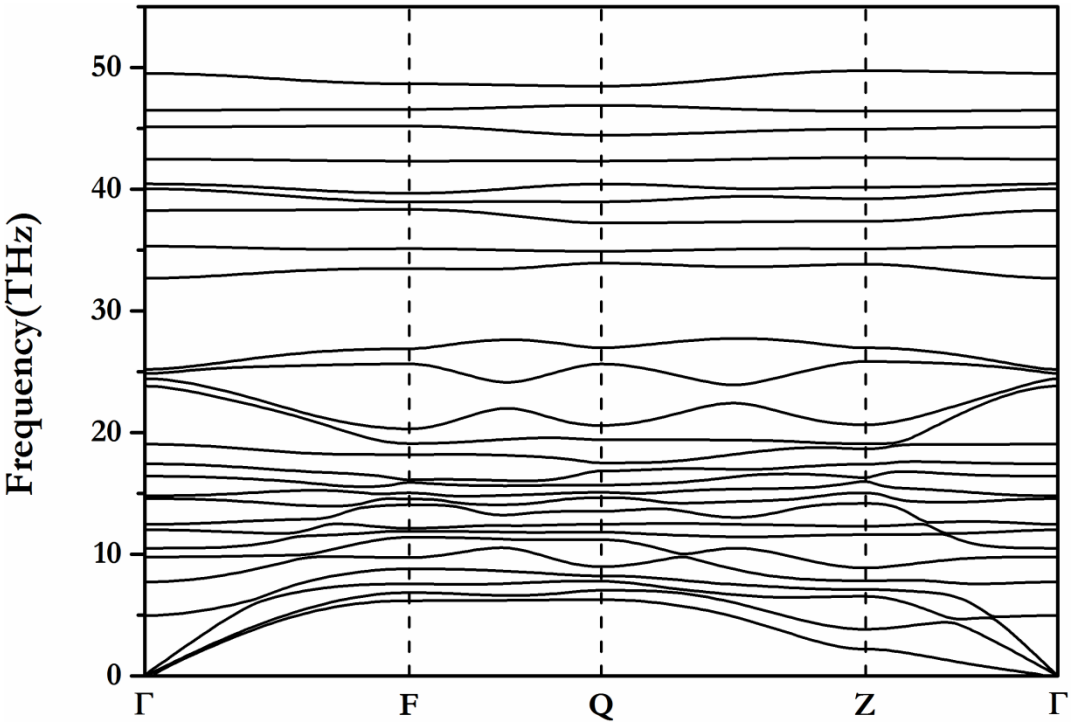

FIG. 8. Phonon dispersion curve of YN_8 in the *P*-1 phase at 75 GPa.

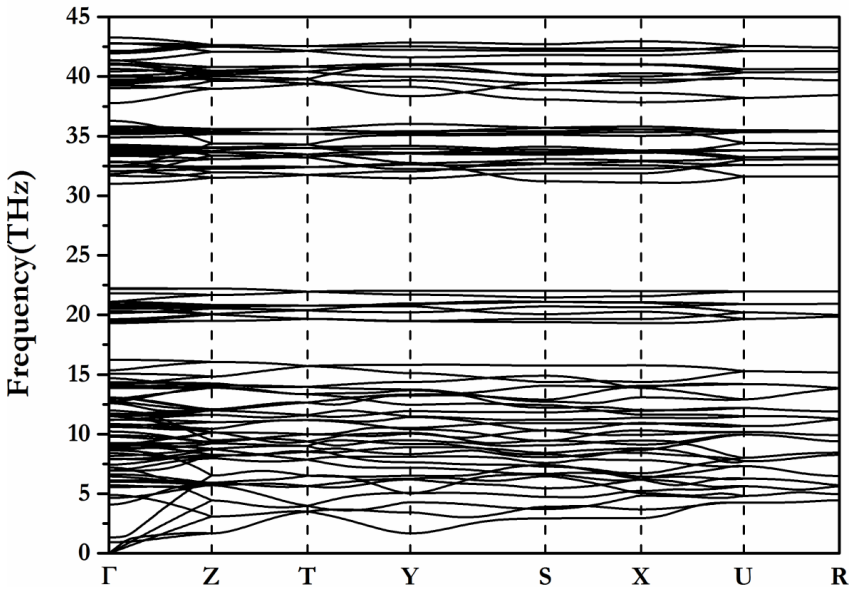

FIG. 9. Phonon dispersion curve of YN_{10} in the *Ibam* phase at 75 GPa.

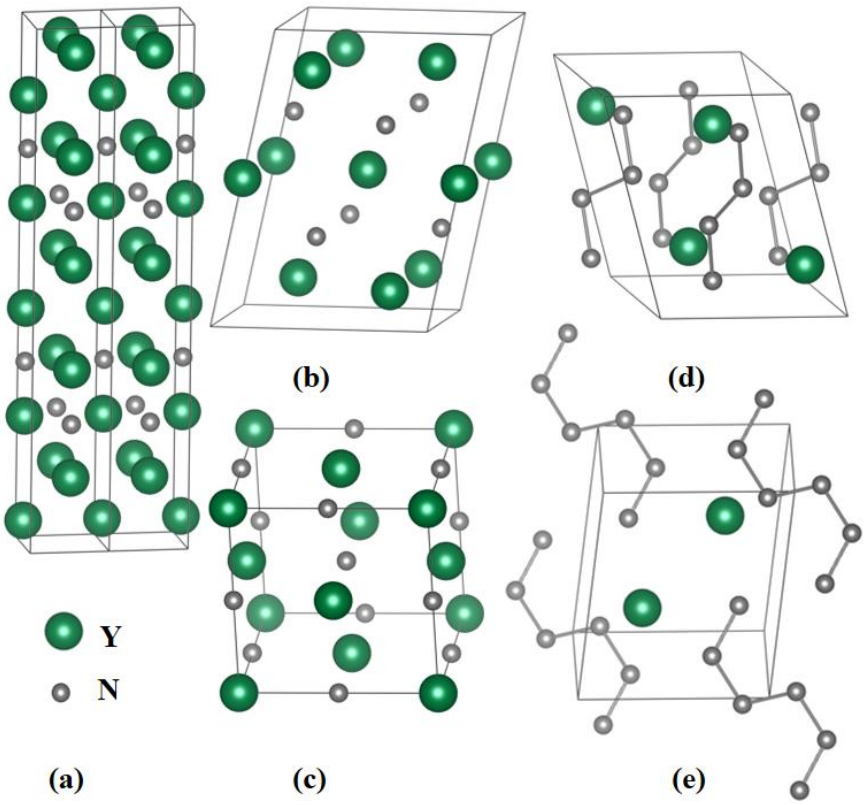

FIG. 10. Crystal structures of polynitrogens for Y-N compounds. (a) *P*4/*nmm* phase for Y_5N_2 at 25 GPa. (b) *C*/2*m* structure for Y_3N_2 at 100 GPa. (c) *Fm*-3*m* structure for YN at 50 GPa. (d) *P*21/*c* phase of YN_2 at 100 GPa. (e) *P*-1 phase of YN_3 at 50 GPa.

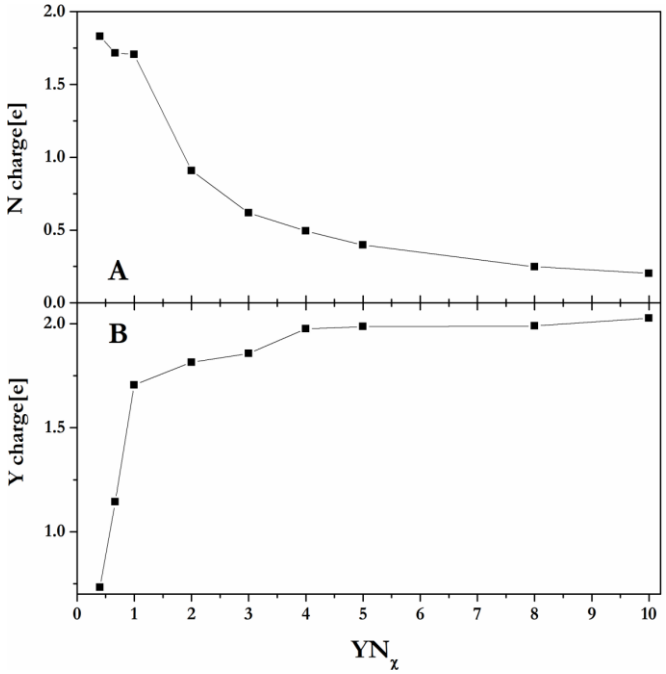

FIG. 11. The calculated cationic and anionic charges of N (A) and Y (B) ions in different YN*x* systems.Bader charge analysis reveals only part of the charges (1.47*e*) of atom transfer to N atom in YN layers and the charges transfer of Y→N are 0.12*e* and 0.31*e* in the double Y layers and quadruple Y layers for Y_5N_2, respectively. Here, we only give the average per atom transfer charges for Y_5N_2.

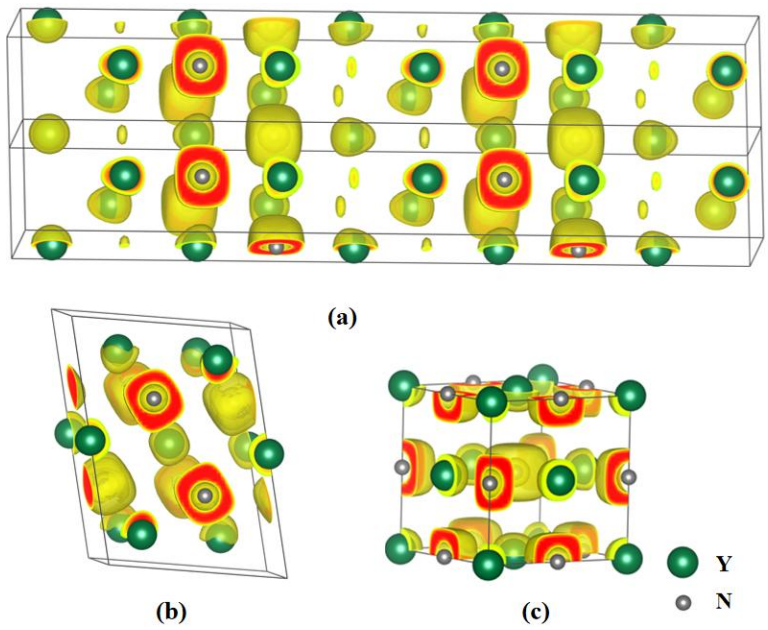

FIG. 12. ELFs for Y-N compounds. (a) *P*4/*nmm* phase for Y_5N_2 at 25 GPa. (b) *C*/2*m* phase for Y_3N_2 at 100 GPa. (c) *Fm*-3*m* phase for YN at 50 GPa.

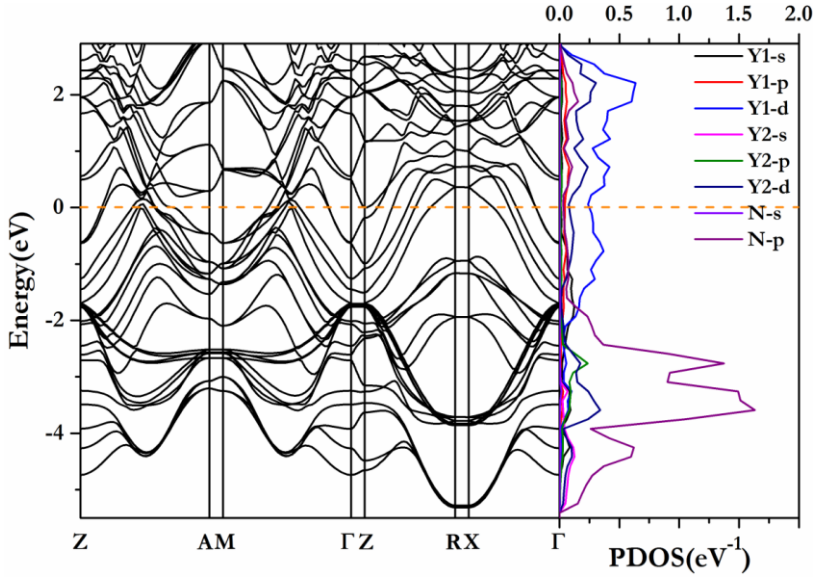

FIG. 13. Electronic band structure and projected DOS per atom of Y1-*s*, Y1-*p*, Y1-*d*, Y2-*s*, Y2-*p*, Y2-*d*, N-*s*, and N-*p* states of P4/*nmm* phase Y_5N_2 at 25 GPa. Y1 is the Y atom in YN layer, and Y2 is the Y atom in Y layer.

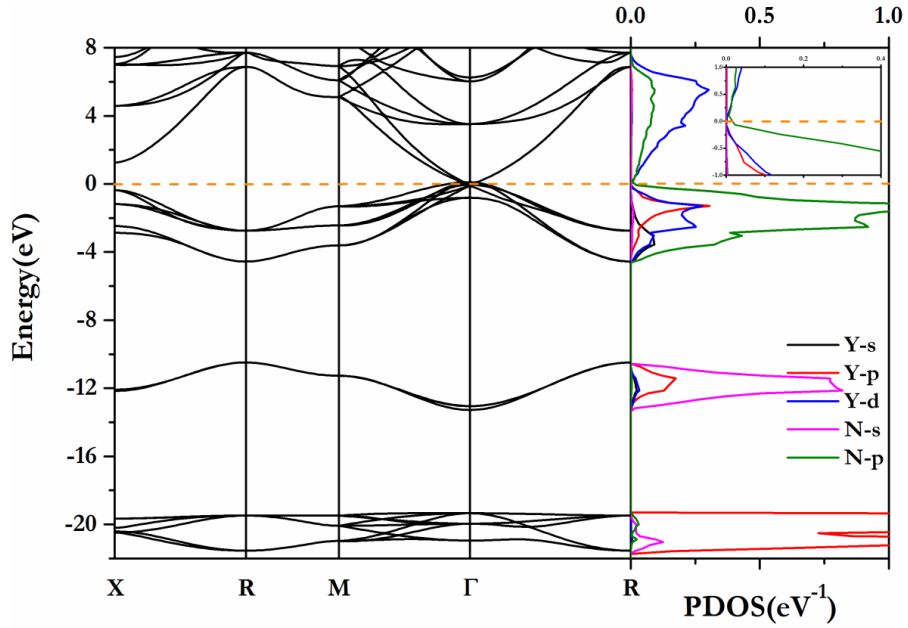

FIG. 14. Electronic band structure and projected DOS per atom of Y-*s*, Y-*p*, Y-*d*, N-*s*, and N-*p* states of *Fm*-3*m* phase YN at 50 GPa. The Y-*d* states at Gamma decompose into e_g and t_{2g} symmetry. The partial DOS also indicates the covalent character due to the fact that Y-*d* and N-*p* PDOS in the occupied parts follow closely with similar weight.

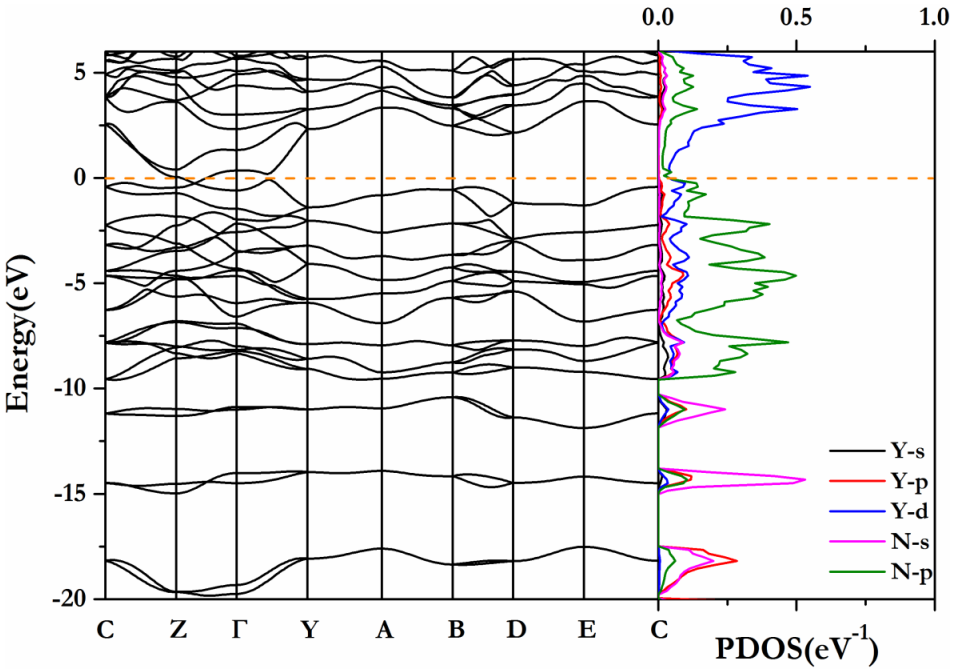

FIG. 15. Electronic band structure and projected DOS per atom of Y-*s*, Y-*p*, Y-*d*, N-*s*, and N-*p* states $P2_1/c$ phase YN_2 at 100 GPa.

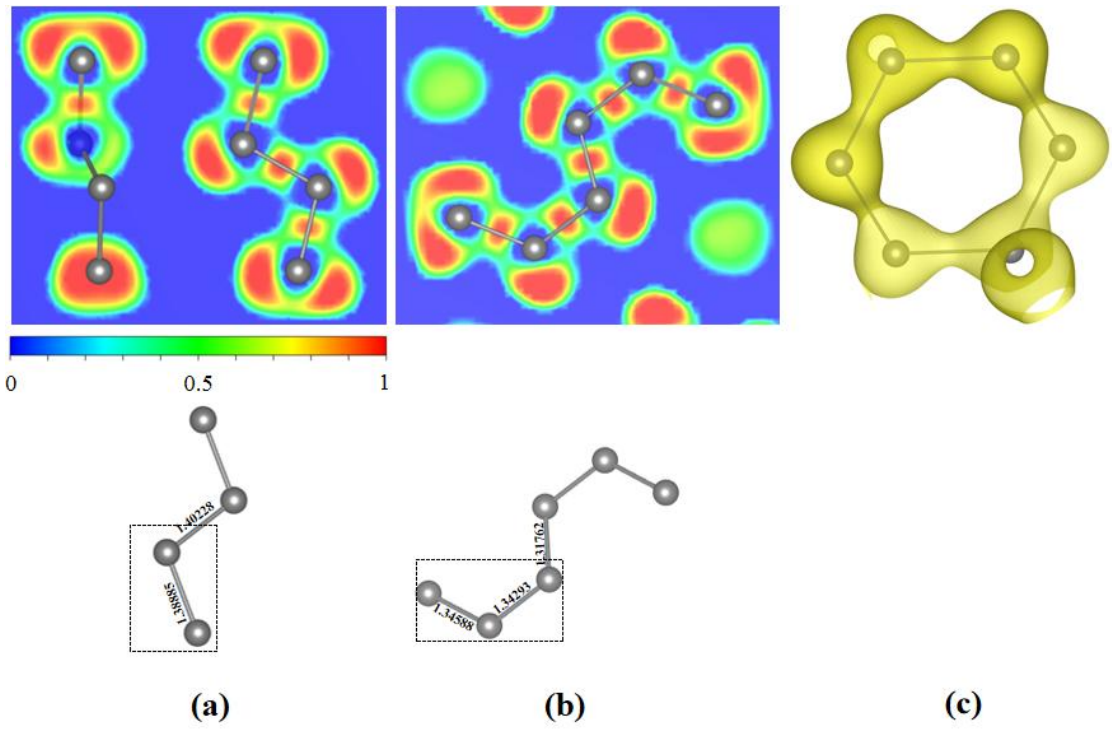

FIG. 16. ELFs and charge densiity of Y-N compounds. (a) *P*21/*c* phase of YN_2 at 100 GPa. The ELF is plotted in (-0.81 -1 0.36) sections for N_4 unit. (b) *P*-1 structure for YN_3 at 50 GPa.The ELF is plotted in (-1 0 -0.68) sections for N_6 unit. (c) The charge densiity of N_6 ring in *C*/2*m* phase of YN_5 at 100 GPa .

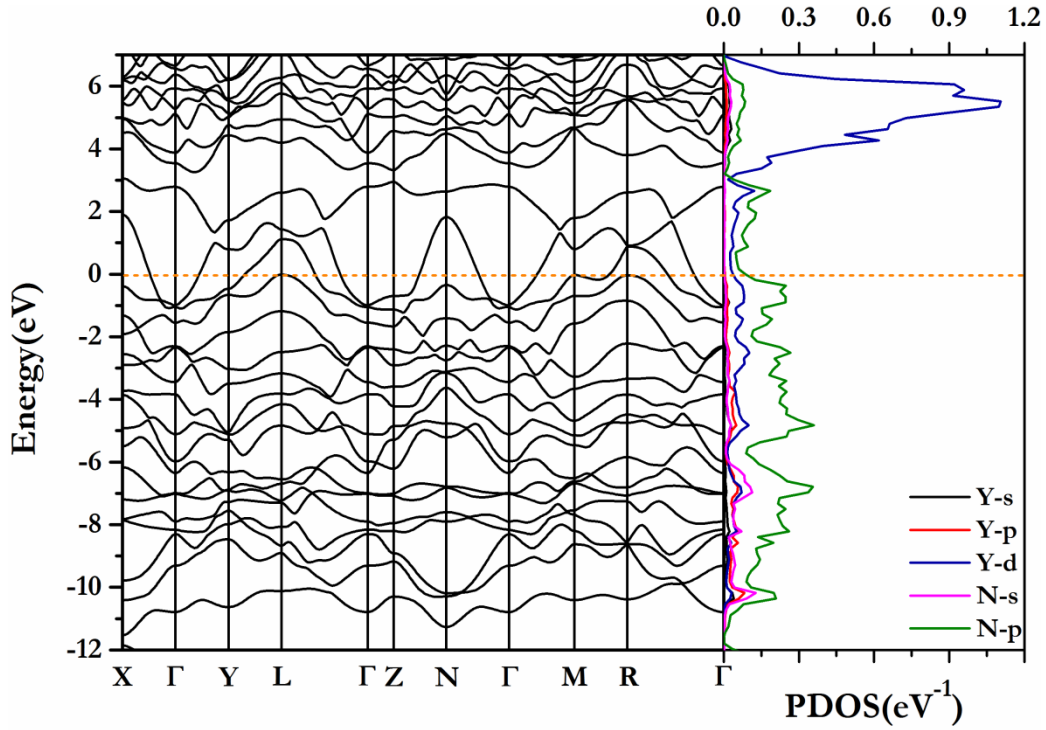

FIG. 17. Electronic band structure and projected DOS per atom of Y-*s*, Y-*p*, Y-*d*, N-*s*, and N-*p* states of *P*-1 phase of YN_4 at 50GPa.

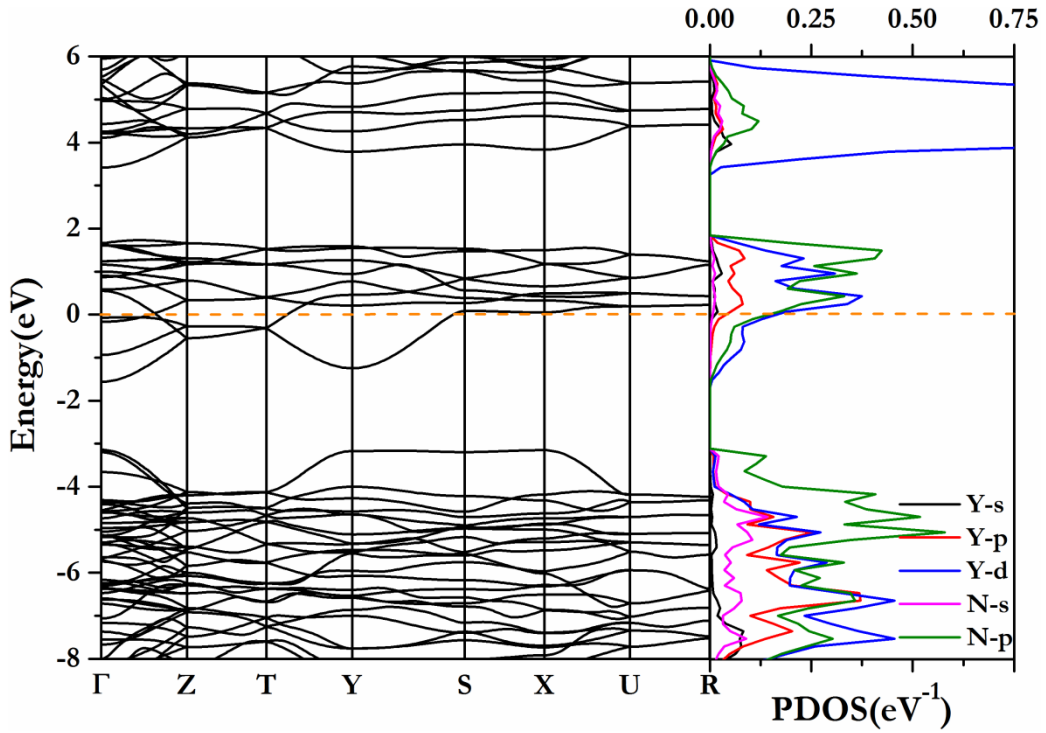

FIG. 18. Electronic band structure and projected DOS per atom of Y-*s*, Y-*p*, Y-*d*, N-*s*, and N-*p* states of the *Ibam* phasee of YN_{10} at 75GPa.

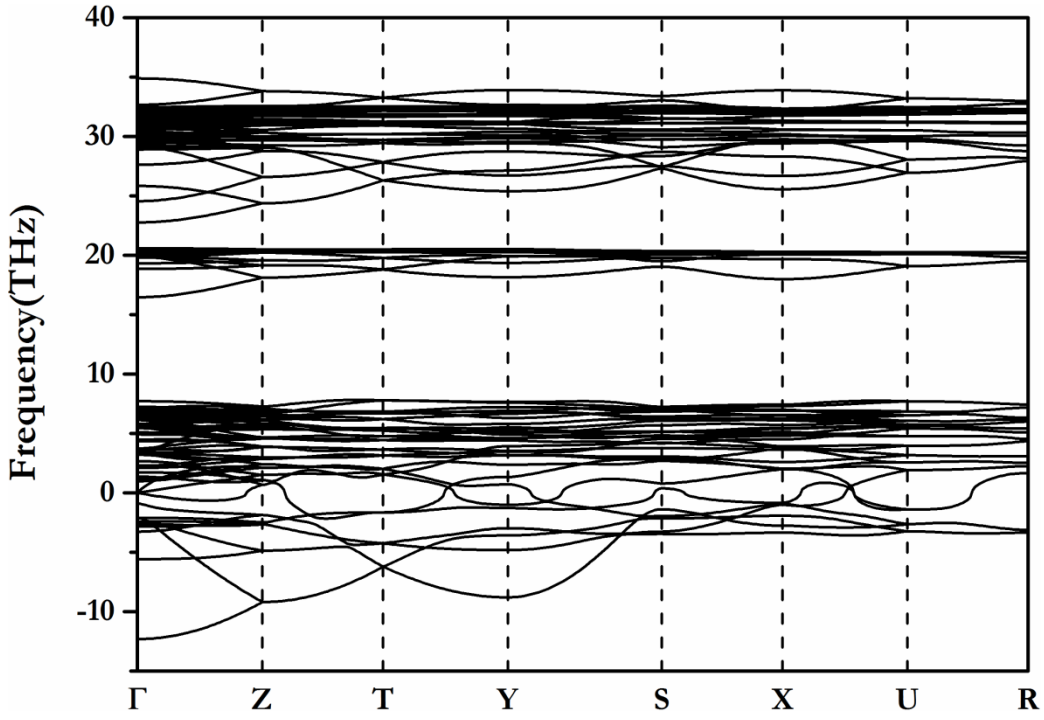

FIG. 19. Phonon dispersion curve of *Ibam* phase YN_{10} at 0 GPa.

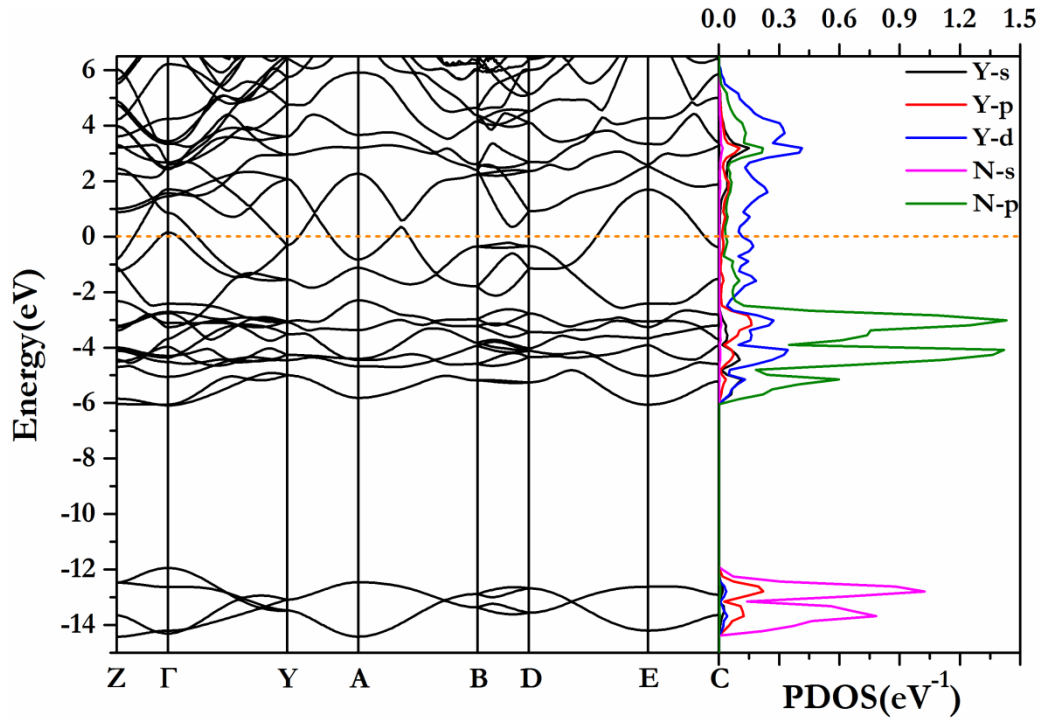

FIG. 20. Electronic band structure and projected DOS per atom of Y-*s*, Y-*p*, Y-*d*, N-*s*, and N-*p* states of *C*/2*m* phase Y_3N_2 at 100GPa.

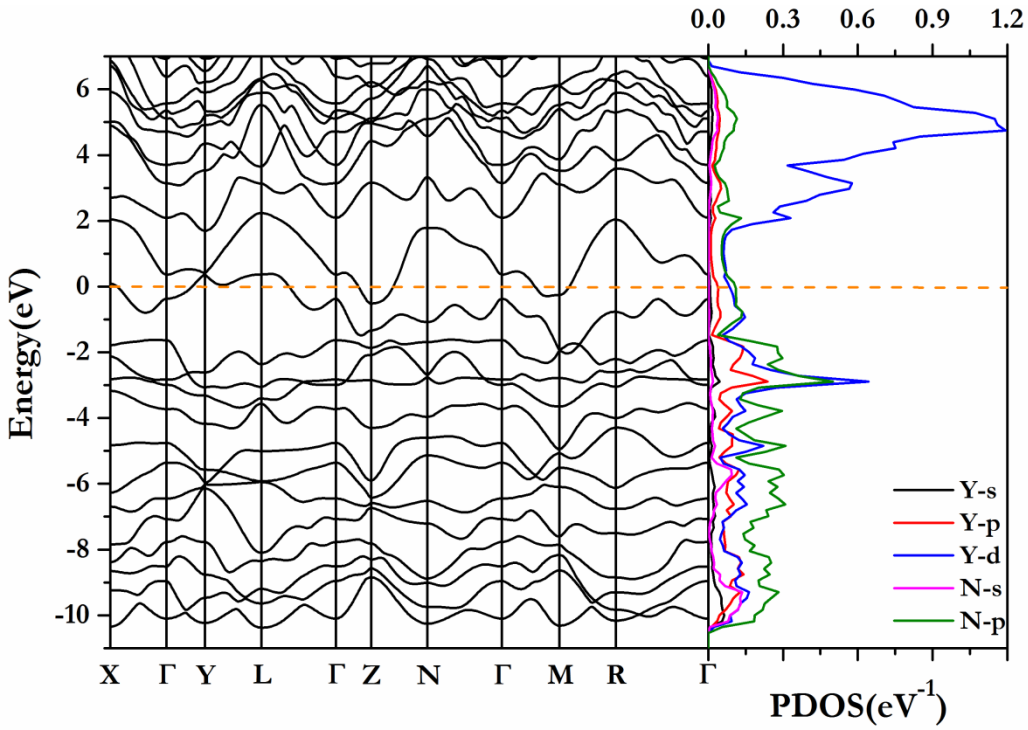

FIG. 21. Electronic band structure and projected DOS per atom of Y-*s*, Y-*p*, Y-*d*, N-*s*, and N-*p* states of *P*-1 phase of YN_3 at 50 GPa.

TABLE I. Calculated structural parameters of various Y-N compounds.

	Space group	lattice parameters *a*, *b*, *c* (Å) *α*, *β*, *γ* (deg)	Atoms	Atomic coordinates (fractional)		
				X	Y	Z
Y_5N_2 (25GPa)	*P4/nmm*	*a*=*b*=3.3154	Y1(2c)	0.50000	0.00000	0.85811
		c=22.1450	Y2(2c)	0.00000	0.50000	0.34819
		α=*β*=*γ*=90.0000	Y3(2c)	0.00000	0.50000	0.54817
			Y4(2c)	0.00000	0.50000	0.95342
			Y5(2c)	0.50000	0.00000	0.24605
			N1(2c)	0.50000	0.00000	0.34982
			N2(2c)	0.50000	0.00000	0.75609
Y_3N_2 (100GPa)	*C*2/*m*	*a*=5.20067	Y1(4i)	0.71138	0.50000	0.13332
		b=3.01959	Y2(2c)	0.00000	0.00000	0.50000
		c=7.20971	N1(4i)	0.60355	0.00000	0.31040
		α=*β*=90.0000				
		γ=103.6652				
YN (50GPa)	*Fm*-3*m*	*a*=*b*=*c*=4.58	Y1(4a)	0.00000	0.00000	0.00000
		α=*β*=*γ*=90.0000	N1(4b)	0.00000	0.50000	0.00000

YN_2	$P2_1/c$	a=5.91050	Y1(4e)	-0.76967	0.47722	-0.11707
(100GPa)		b= 4.42080	N1(4e)	-0.17391	0.02773	0.14925
		c=4.39840	N5(4e)	-0.43333	0.08439	-0.06693
		α=γ=90.0000				
		β=118.4491				
YN_3	P-1	a= 3.11250	Y1(2i)	0.58177	0.69281	0.30482
(50GPa)		b= 4.45580	N1(2i)	0.73189	0.19888	0.36202
		c=4.87550	N2(2i)	0.11071	0.68105	0.83070
		α=99.4988	N3(2i)	0.99749	0.13661	0.96963
		γ=106.3797				
		β= 101.0410				
YN_4	P-1	a= 3.53080	Y1(2i)	0.93742	0.26205	0.72095
(50GPa)		b= 3.60790	N1(2i)	0.36742	0.05172	0.04786
		c=7.10240	N2(2i)	0.35627	0.40938	0.04681
		α=104.1765	N3(2i)	0.72693	0.16915	0.38451
		γ=94.6326	N4(2i)	0.49839	0.40868	0.40707
		β= 106.9361				
YN_5	$C2/m$	a=6.79170	Y1(4h)	0.00000	0.76914	0.50000
(100GPa)		b= 7.04290	N1(8j)	0.88007	0.33681	0.33681
		c= 7.04290	N2(4i)	0.71819	0.00000	0.10381
		α=γ=90.0000	N3(4i)	0.29503	0.00000	0.24716
		β=123.1281	N4(4i)	0.91632	0.00000	0.82301

TABLE II. Calculated structural parameters of various Y-N compounds.

	Space group	**lattice parameters** ***a, b, c* (Å)*α, β, γ* (deg)**	**Atoms**	**Atomic coordinates (fractional)**		
				X	**Y**	**Z**
YN_8	P-1	a= 3.51660	Y1(1d)	0.50000	0.50000	0.00000
(75GPa)		b= 3.71620	N1(2i)	0.19296	0.71884	0.36967
		c=5.09080	N2(2i)	0.62164	0.41220	0.44212
		α=104.0308	N3(2i)	0.82854	0.45677	0.89652
		γ=101.6472	N4(2i)	0.09158	0.11361	0.11361
		β= 100.6977				
YN_{10}	*Ibam*	a= 7.79730	Y1(4a)	0.00000	0.00000	0.25000
(75GPa)		b= 5.51150	N1(16k)	0.88451	0.34289	0.14622
		c=7.25370	N2(8j)	0.52563	0.77617	0.00000
		α=β=γ=90.0000	N3(16k)	0.74878	0.44784	0.91136

TABLE III. Elastic constants C_{ij} (GPa), bulk modulus B(GPa), shear modulus G(GPa), Young's modulus E(GPa), and Possion's ratio v of P-1-YN_4, $C2/m$-YN_5, P-1-YN_8, and $Ibam$-YN_{10} at ambient pressure.

		C_{11}	C_{22}	C_{33}	C_{44}	C_{55}	C_{66}	C_{12}	C_{13}	C_{14}	C_{15}	C_{16}
YN_4	*P*-1	171	371	259	72	72	29	73	58	19	10	15
YN_8	*P*-1	172	497	239	103	139	148	57	158	22	25	91
		C_{23}	C_{24}	C_{25}	C_{26}	C_{34}	C_{35}	C_{36}	C_{45}	C_{46}	C_{56}	
YN_4	*P*-1	68	71	1	12	10	-1	42	11	4	16	
YN_8	*P*-1	82	60	-49	30	-6	25	135	86	14	10	
		B	*G*	*E*	*v*							
YN_4	*P*-1	113	60	153	0.27							
YN_8	*P*-1	126	77	192	0.25							
		C_{11}	C_{22}	C_{33}	C_{44}	C_{55}	C_{66}	C_{12}	C_{13}	C_{15}	C_{23}	C_{25}
YN_5	*C*2/*m*	353	221	73	52	126	53	36	149	-43	40	15
YN_{10}	*Ibam*	122	61	95	-56	-171	25	56	42		18	
		C_{35}	C_{46}	*B*	*G*	*E*	*v*					
YN_5	*C*2/*m*	-34	11	70	42	105	0.25					
YN_{10}	*Ibam*			51	7	20	0.43					

Note:

For a monoclinic phase, the criteria for mechanical stability are given by the following equation:

$$C_{11}>0,\quad C_{22}>0,\quad C_{33}>0,\quad C_{44}>0,\quad C_{55}>0,$$
$$C_{66}>0,\quad [C_{11}+C_{22}+C_{33}+2(C_{12}+C_{13}+C_{23})]>0,$$
$$(C_{33}C_{55}-C_{35}^2)>0,\quad (C_{44}C_{66}-C_{46}^2)>0,$$
$$(C_{22}+C_{33}-2C_{23})>0,$$
$$[C_{22}(C_{33}C_{55}-C_{35}^2)+2C_{23}C_{25}C_{35}-C_{23}^2C_{55}-C_{25}^2C_{33}]>0,$$
$$\{2[C_{15}C_{25}(C_{33}C_{12}-C_{13}C_{23})+C_{15}C_{35}(C_{22}C_{13}-C_{12}C_{23})+C_{25}C_{35}(C_{11}C_{23}-C_{12}C_{13})]-[C_{15}^2(C_{22}C_{33}-C_{23}^2)+C_{25}^2(C_{11}C_{33}-C_{13}^2)+C_{35}^2(C_{11}C_{22}-C_{12}^2)]+C_{55}g\}>0.$$

Here $g=C_{11}C_{22}C_{33}-C_{11}C_{23}^2-C_{22}C_{13}^2-C_{33}C_{12}^2+2C_{12}C_{13}C_{23}$

For an orthorhombic phase, the criteria for mechanical stability are given by the following equation:

$$C_{11}>0,\quad C_{22}>0,\quad C_{33}>0,\quad C_{44}>0,\quad C_{55}>0,$$
$$C_{66}>0,\quad [C_{11}+C_{22}+C_{33}+2(C_{12}+C_{13}+C_{23})]>0,$$
$$(C_{11}+C_{22}-2C_{12})>0,\quad (C_{11}+C_{33}-2C_{13})>0,$$
$$(C_{22}+C_{33}-2C_{23})>0.$$